manuscript No.
(will be inserted by the editor)

Improved Fast Gauss Transfom for meshfree ElectroMagnetic transients simulations

Elisa Francomano · Guido Ala · Marta Paliaga

Received: February 7 2019

Abstract In this paper improved fast summations are introduced to enhance a meshfree solver for the evolution of the electromagnetic fields over time. The original method discretizes the time-domain Maxwell's curl equations via Smoothed Particle Hydrodynamics requiring many summations on the first derivatives of the kernel function and field vectors at each time step. The improved fast Gauss transform is properly adopted picking up the computational cost and the memory requirement at an acceptable level preserving the accuracy of the computation. Numerical simulations in two-dimensional domains are discussed giving evidence of improvements in the computation compared to the standard formulation.

Keywords Numerical Approximation · Improve Fast Gauss Transform · Smoothed Particle Hydrodynamics · Maxwell's equations

1 Introduction

Despite the success of the mesh based methods in the analysis of widely areas of the engineering and physical science a number of faults in handling physical problems occurs involving large deformations, high gradients or moving discontinuities. Recently, the new generation of so-called meshfree methods has emerged and is profoundly influencing many branches of applied science [4,6,7,12]. One of the most distinguished feature about these methods is that no explicit mesh is needed in the formulation. As a part of this family,the Smoothed Particle Hydrodynamics

E.Francomano
University of Palermo, Department of Engineering, Numerical Analysis
Tel.:+3909123862629
E-mail: elisa.francomano@unipa.it

G. Ala
University of Palermo, Department of Engineering, Electrical Engineering
E-mail: guido.ala@unipa.it

M. Paliaga
University of Palermo, Department of Engineering, Numerical Analysis
E-mail: marta.paliaga@unipa.it

(SPH) method, developed by Gingold, Monaghan [8] and Lucy [13] in 1977 to analyze astrophysical problems, has been later adopted in various areas of science and engineering [5,10,11,14,16]. It has shown very appropriate in computational electromagnetics too and produces results comparable to those obtained with the Finite Difference Time Domain (FDTD) method [19], which can be assumed representative of conventional techniques used in practice. The authors applied the method in simulating electromagnetics transients [1–3]. Nevertheless, in discretizing time-domain Maxwell's curl equations many summations are required on the first derivatives of the kernel functions marching on in time. By adopting the Gaussian kernel the function is itself a common element for all order derivatives,allowing us to adopt the improved fast Gauss transform (IFGT) [17,18] for all the summations to reduce the computational cost while preserving the required accuracy. The reduction is based on the multivariate Taylor's series expansion scheme combined with an efficient space subdivision scheme achieving linear complexity. We find it interesting and show it can lead to good performance in simulating electric and magnetic fields propagation. The remainder of the paper is as follows. In section 2 we present the standard formulation of the method in the computational electromagnetic context. In section 3 we present the basic ideas underlying the improved fast Gauss transform and its application into the EM framework. Finally in section 4 we propose a numerical test case for the two-dimensional EM propagation dealt with both the standard and the fast computation via improved fast Gauss transform, comparing the results with the FDTD solver. In this manuscript we present first results with the intent to extend in the future research the proposed approach to model in a fast and accurate fashion the effects of electromagnetic radiation on human tissue for safety and for accurate real-time therapeutic applications.

2 The Smoothed Particle Hydrodynamics for EM simulations

In this section we shortly present the standard SPH method embedded in a computational electromagnetic context. The interested reader is directed to [11,12] for a more expository treatment of the method. Two key steps usually named as *kernel approximation* and *particle approximation* characterize the method.
The first step approximates a function $f : \Omega \subset \mathbb{R}^d \to \mathbb{R}$, $d \in N, d \geq 1$, by means of

$$< f_h(\mathbf{x}) >:= \int_\Omega f(\boldsymbol{\xi}) \mathsf{K}(\mathbf{x}, \boldsymbol{\xi}; h) d\Omega \tag{1}$$

with $\mathbf{x} = (x^{(1)}, ..., x^{(d)})$, $\boldsymbol{\xi} = (\xi^{(1)}, ..., \xi^{(d)}) \in \Omega$, $h \in \mathbb{R}$.
Given a finite point set $\Xi = \{\boldsymbol{\xi}_j\}_{j=1}^N \subset \Omega$ and $\{y_j = f(\boldsymbol{\xi}_j)\}_{j=1}^N \in \mathbb{R}$, the *particle approximation* is defined as

$$f_h(\mathbf{x}) := \sum_{j=1}^N f(\boldsymbol{\xi}_j) \mathsf{K}(\mathbf{x}, \boldsymbol{\xi}_j; h) d\Omega_j \tag{2}$$

where $d\Omega_j$ is the measure of the subdomain Ω_j associated with each point.
Our experience concerns the time-dependent Maxwell's curl equations

$$\nabla \times \mathbf{H} = \epsilon \partial_t \mathbf{E} + \sigma \mathbf{E}, \qquad \nabla \times \mathbf{E} = -\mu \partial_t \mathbf{H}$$

which describe the coupled behavior of the electric $\mathbf{E}$ and the magnetic field $\mathbf{H}$ and the interactions with surrounding objects with the permittivity ϵ, the permeability μ and the conductivity σ assumed constant in time. The physical laws depend on the field variables in time and space and in the Cartesian coordinate systems the equations are conducted to the following *first order* time-domain equations

$$\partial_t \mathbf{E}_\alpha(\mathbf{x},t) = \frac{1}{\epsilon}[\partial_\beta \mathbf{H}_\gamma(\mathbf{x},t) - \partial_\gamma \mathbf{H}_\beta(\mathbf{x},t) - \sigma \mathbf{E}_\alpha(\mathbf{x},t)] \quad (3)$$

$$\partial_t \mathbf{H}_\alpha(\mathbf{x},t) = -\frac{1}{\mu}[\partial_\beta \mathbf{E}_\gamma(\mathbf{x},t) - \partial_\gamma \mathbf{E}_\beta(\mathbf{x},t)] \quad (4)$$

$$\alpha = x,y,z; \beta = y,z,x; \gamma = z,x,y.$$

The scheme is applied with a geometrical pattern that staggers points where the magnetic and the electric field components are stored in separate locations. The electric field$\mathbf{E}$ is computed at the points $\Xi^E = \left\{\boldsymbol{\xi}_j^E\right\}_{j=1}^{N_E} whilethemagneticfield \mathrm{H} at \Xi^H = \left\{\boldsymbol{\xi}_j^H\right\}_{j=1}^{N_H}$ respectively. By adopting the particle approximation in (3) and (4) we obtain

$$\partial_t \mathbf{E}_\alpha(\boldsymbol{\xi}_i^E,t) = \frac{1}{\epsilon}\sum_{\boldsymbol{\xi}_j^H \in \Omega} [\mathbf{H}_\gamma(\boldsymbol{\xi}_j^H,t)\partial_\beta - \mathbf{H}_\beta(\boldsymbol{\xi}_j^H,t)\partial_\gamma]\mathsf{K}_{ij}^E d\Omega_j - \frac{\sigma}{\epsilon}\mathbf{E}_\alpha(\boldsymbol{\xi}_i^E,t) \quad (5)$$

$$\partial_t \mathbf{H}_\alpha(\boldsymbol{\xi}_i^H,t) = -\frac{1}{\mu}\sum_{\boldsymbol{\xi}_j^E \in \Omega} [\mathbf{E}_\gamma(\boldsymbol{\xi}_j^E,t)\partial_\beta - \mathbf{E}_\beta(\boldsymbol{\xi}_j^E,t)\partial_\gamma]\mathsf{K}_{ij}^H d\Omega_j \quad (6)$$

$\alpha = x,y,z; \beta = y,z,x; \gamma = z,x,y;$ $\mathsf{K}_{ij}^E = \mathsf{K}(\boldsymbol{\xi}_i^E,\boldsymbol{\xi}_j^H;h)$; $\mathsf{K}_{ij}^H = \mathsf{K}(\boldsymbol{\xi}_i^H,\boldsymbol{\xi}_j^E;h)$.

A time-domain solver takes the Maxwell's equations with time derivatives into account and yields the solution marching on in time with a given step. The time domain is discretized in a straightforward manner by splitting the time into constant intervals Δt and the field components are placed in a staggered fashion in time. The magnetic field values are stored at full time steps while the electric field values at the intermediate half steps.
The final formulation with the explicit update equations for the cartesian set up is considered and gives rise to the following evolution in time

$$\mathbf{E}_\alpha^{(n+1/2)}(\boldsymbol{\xi}_i^E) = \mathbf{E}_\alpha^{(n-1/2)}(\boldsymbol{\xi}_i^E) + \frac{\Delta t}{\epsilon}\sum_{\boldsymbol{\xi}_j^H \in \Omega} [\mathbf{H}_\gamma^{(n)}(\boldsymbol{\xi}_j^H)\partial_\beta +$$

$$-\mathbf{H}_\beta^{(n)}(\boldsymbol{\xi}_j^H)\partial_\gamma]\mathsf{K}_{ij}^E d\Omega_j - \frac{\sigma\Delta t}{\epsilon}\mathbf{E}_\alpha^{(n-1/2)}(\boldsymbol{\xi}_i^E) \quad (7)$$

$$\mathbf{H}_\alpha^{(n+1)}(\boldsymbol{\xi}_i^H) = \mathbf{H}_\alpha^{(n)}(\boldsymbol{\xi}_i^H) - \frac{\Delta t}{\mu}\sum_{\boldsymbol{\xi}_j^E \in \Omega} [\mathbf{E}_\gamma^{(n+1/2)}(\boldsymbol{\xi}_j^E)\partial_\beta - \mathbf{E}_\beta^{(n+1/2)}(\boldsymbol{\xi}_j^E)\partial_\gamma]\mathsf{K}_{ij}^H d\Omega_j \quad (8)$$

$$\alpha = x,y,z; \beta = y,z,x; \gamma = z,x,y.$$

3 Improved Fast Gauss Transform for the EM solver

3.1 Fundamental of the fast summation

By adopting the smooth and infinitely differentiable Gaussian as kernel function we make use of the improved fast Gauss transform (IFGT) [17,18] for all the summations in (7) and (8). In this way the original fast Gauss transform by Greengard and Strain [9] is considerably improved both in term of computational cost and in accuracy. In computing

$$G(\mathbf{x}_i) = \sum_{j=1}^{N} w_j e^{-\frac{\|\mathbf{x}_i - \boldsymbol{\xi}_j\|^2}{h^2}} \qquad i = 1, ..., M, \tag{9}$$

w_j as the weight coefficients and $\{\mathbf{x}_i\}_{i=1}^{M} \subseteq \mathbb{R}^d$ as the evaluation points, the IFGT re-writes the exponential term as

$$e^{-\frac{\|\mathbf{x}_i - \boldsymbol{\xi}_j\|^2}{h^2}} = e^{-\frac{\|\mathbf{x}_i - \mathbf{x}^*\|^2}{h^2}} e^{-\frac{\|\boldsymbol{\xi}_j - \mathbf{x}^*\|^2}{h^2}} e^{\frac{2(\boldsymbol{\xi}_j - \mathbf{x}^*)(\mathbf{x}_i - \mathbf{x}^*)}{h^2}}. \tag{10}$$

The first two terms in (10) can be computed independently while remains a problem with the term where $\mathbf{x}_i$ and the $\boldsymbol{\xi}_j$ are entangled. To solve this question the multivariate Taylor series expansion centered at location $\mathbf{x}^*$ ~~,~~ is considered

$$\hat{G}(\mathbf{x}_i) = e^{-\frac{\|\mathbf{x}_i - \mathbf{x}^*\|^2}{h^2}} \sum_{|\alpha| \le k-1} \mathcal{C}_\alpha \left(\mathbf{x}_i - \mathbf{x}^*\right)^\alpha \tag{11}$$

with

$$C_\alpha = \frac{2^{|\alpha|}}{\alpha!} \sum_{j=1}^{N} w_j e^{-\frac{\|\boldsymbol{\xi}_j - \mathbf{x}^*\|^2}{h^2}} \left(\frac{\boldsymbol{\xi}_j - \mathbf{x}^*}{h^2}\right)^\alpha .$$

Considering the rapidly decreasing of the Gaussian function, the space is divided into cells, collecting the influences of the $\boldsymbol{\xi}_j$. In this way, by choosing a "cut-off" radius r_x for each evaluation point, only the cells lying within r_x are taking into account in the summation. To this aim the N points $\boldsymbol{\xi}_j$ are divided into p sets $S_1, ..., S_p$ with $c_1, ..., c_p$ the p centers respectively. After the partition is completed, the truncation number k is chosen for each cell, in order to obtain the precision required. For each $p-$th cell with center c_p

$$\mathcal{C}_\alpha^p = \frac{2^{|\alpha|}}{\alpha!} \sum_{\boldsymbol{\xi}_j \in S_p} w_j e^{-\frac{\|\boldsymbol{\xi}_j - \mathbf{c}_p\|^2}{h^2}} \left(\frac{\boldsymbol{\xi}_j - \mathbf{c}_p}{h}\right)^\alpha \tag{12}$$

and for each evaluation point $\mathbf{x}_i$ the fast summation is found as

$$\hat{G}(\mathbf{x}_i) = \sum_{\|\mathbf{x}_i - \mathbf{c}_p\| \le r_x} \sum_{|\alpha| \le k-1} \mathcal{C}_\alpha^p e^{-\frac{\|\mathbf{x}_i - \mathbf{c}_p\|^2}{h^2}} \left(\frac{\mathbf{x}_i - \mathbf{c}_p}{h}\right)^\alpha . \tag{13}$$

For more details on the process the reader is invited to refer to [17,18].

3.2 IFGT and EM solver

The fast summation IFGT is employed into the EM meshfree solver in which the linear combination of the first order derivatives of Gaussian and the vector fields is the key computational task. By considering that the first Gaussian derivatives employ the function itself

$$\partial_s e^{-\frac{\|\mathbf{x}_i-\boldsymbol{\xi}_j\|^2}{h^2}} = -\frac{2}{\pi h^2}(x_i^{(s)} - \xi_j^{(s)})e^{-\frac{\|\mathbf{x}_i-\boldsymbol{\xi}_j\|^2}{h^2}} \tag{14}$$

we deal with summations as

$$G(\mathbf{x}_i) = \sum_{j=1}^{N} \omega_j (x_i^{(s)} - \xi_j^{(s)})e^{-\frac{\|\mathbf{x}_i-\boldsymbol{\xi}_j\|^2}{h^2}} \quad i = 1, ..., M, \tag{15}$$

where ω_j are the weights which depend on the smoothing length h, on the magnetic or the electric field evaluated at $\boldsymbol{\xi}_j^E$ and $\boldsymbol{\xi}_j^H$ respectively and the measure of the related subdomains.
Therefore, two fast summations $G_1(\mathbf{x}_i)$ and $G_2(\mathbf{x}_i)$ are detected inside(15)

$$G(\mathbf{x}_i) = x_i^{(s)} G_1(\mathbf{x}_i) + G_2(\mathbf{x}_i) = x_i^{(s)} \sum_{j=1}^{N} \omega_j e^{-\frac{\|\mathbf{x}_i-\boldsymbol{\xi}_j\|^2}{h^2}} - \sum_{j=1}^{N} (\omega_j \xi_j^{(s)}) e^{-\frac{\|\mathbf{x}_i-\boldsymbol{\xi}_j\|^2}{h^2}}. \tag{16}$$

At this time, it is evident that we can update the electric field $\mathbf{E}_\alpha$ and the magnetic field $\mathbf{H}_\alpha$ by making use of IFGTs in each of the following summations

$$G_{\mathbf{E}_\alpha}(\boldsymbol{\xi}_i^E)^{(1)} = \frac{1}{\epsilon} \sum_{j=1}^{N_H} [\mathbf{H}_\gamma^{(n)}(\boldsymbol{\xi}_j^H) d\Omega_j] \partial_\gamma e^{-\frac{\|\boldsymbol{\xi}_i^E-\boldsymbol{\xi}_j^H\|^2}{h^2}} \qquad i = 1, ..., N_E,$$

$$G_{\mathbf{E}_\alpha}(\boldsymbol{\xi}_i^E)^{(2)} = \frac{1}{\epsilon} \sum_{j=1}^{N_H} [\mathbf{H}_\beta^{(n)}(\boldsymbol{\xi}_j^H) d\Omega_j] \partial_\beta e^{-\frac{\|\boldsymbol{\xi}_i^E-\boldsymbol{\xi}_j^H\|^2}{h^2}} \qquad i = 1, ..., N_E,$$

$$G_{\mathbf{H}_\alpha}(\boldsymbol{\xi}_i^H)^{(1)} = -\frac{1}{\mu} \sum_{j=1}^{N_E} [\mathbf{E}_\gamma^{(n+1/2)}(\boldsymbol{\xi}_j^E) d\Omega_j] \partial_\beta e^{-\frac{\|\boldsymbol{\xi}_i^H-\boldsymbol{\xi}_j^E\|^2}{h^2}} \quad i = 1, ..., N_H,$$

$$G_{\mathbf{H}_\alpha}(\boldsymbol{\xi}_i^H)^{(2)} = -\frac{1}{\mu} \sum_{j=1}^{N_E} [\mathbf{E}_\beta^{(n+1/2)}(\boldsymbol{\xi}_j^E) d\Omega_j] \partial_\gamma e^{-\frac{\|\boldsymbol{\xi}_i^H-\boldsymbol{\xi}_j^E\|^2}{h^2}} \quad i = 1, ..., N_H.$$

4 Numerical results

In this section we discuss on two-dimensional EM propagation. We consider the transverse mode (TM) involving the vector fields $\mathbf{E}_z, \mathbf{H}_x, \mathbf{H}_y$, with σ=0 and described by the equations

$$\partial_t \mathbf{E}_z(\mathbf{x}, t) = \frac{1}{\epsilon}[\partial_y \mathbf{H}_x(\mathbf{x}, t) - \partial_x \mathbf{H}_y(\mathbf{x}, t)] \tag{17}$$

$$\partial_t \mathbf{H}_x(\mathbf{x}, t) = -\frac{1}{\mu}[\partial_y \mathbf{E}_z(\mathbf{x}, t)] \tag{18}$$

$$\partial_t \mathbf{H}_y(\mathbf{x}, t) = -\frac{1}{\mu}[\partial_x \mathbf{E}_(\mathbf{x}, t)]. \tag{19}$$

A Gaussian pulse source is generated in the middle of the problem space and it travels outward. We'll look at the behavior of electric and magnetic field far away from the source. In the Figs. 1,2,3 the propagation of the fields, obtained by adopting the SPH approach with $N_E = N_H = 3600$ points located in a uniform fashion throughout in Ω, is depicted at different iteration steps T.Various simulations are conducted by increasing the number of the **E**-points and the **H**-points in the problem domain. In order to assess the method we compare it with the FDTD solver and the Root Mean Square Error (RMSE) is used in the validation.

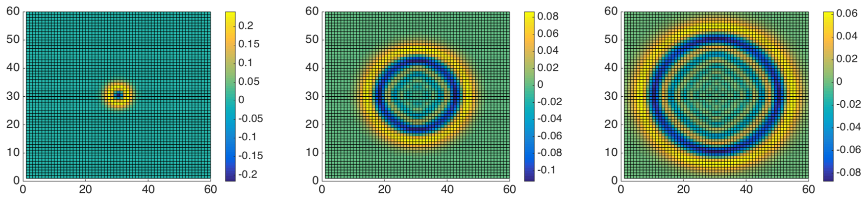

(a) T=5 (b) T=30 (c) T=45

Fig. 1 Magnitude of the $\mathbf{E}_z$vector field with $N_E = N_H = 3600$ at different iteration steps T.

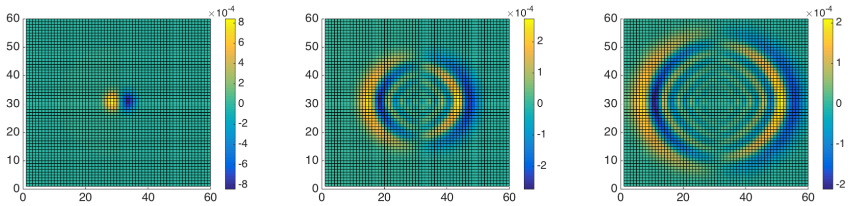

(a) T=5 (b) T=30 (c) T=45

Fig. 2 Magnitude of the $\mathbf{H}_x$vector field with $N_E = N_H = 3600$ at different iteration steps T.

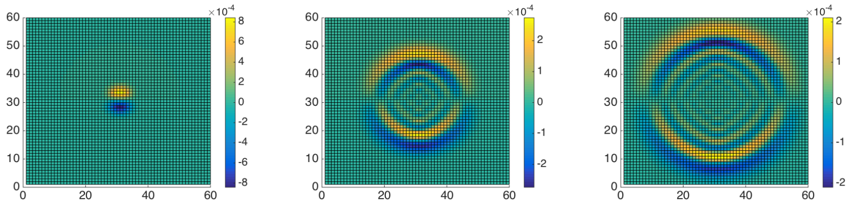

(a) T=5 (b) T=30 (c) T=45

Fig. 3 Magnitude of the $\mathbf{H}_y$vector field with $N_E = N_H = 3600$ at different iteration steps T.

In Fig.4 we depict the RMSE for the marching on in time of the vector field $\mathbf{E}_z$ by varying $N_E = N_H \in [100, 8100]$. The method performs well with high values of N_E but it is computationally demanding as we can observe in the Table 1 showing the running time (sec.) as the number of data increases. In the same table are reported the running times by adopting the IFGTs in all the summations employed in the computation at a single time step giving evidence of the improvements with high number of data sites. The algorithm is programmed in MATLAB and was run on a computer equipped with a processor Intel(R) Core(TM) i7-3537U CPU 2.00GHz.

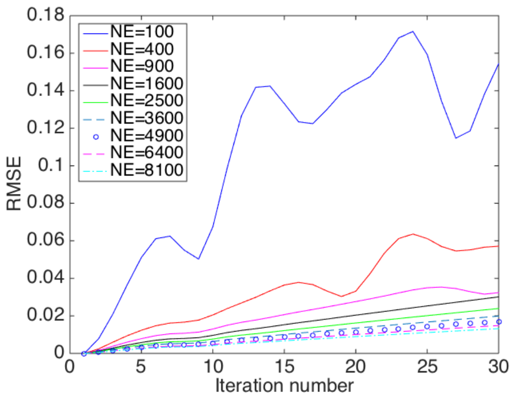

Fig. 4 RMSE for the marching on in time of $\mathbf{E}_z$ by increasing the total number N_E=N_H of **E**-points and **H**-points.

Table 1 Running times (sec.) for a time step with the standard formulation and IFGT respectively.

N_E	400	900	1600	2500	3600	4900	6400
Standard	0.0165	0.0297	0.4900	1.6816	3.0235	12.4617	59.6142
IFGT	0.0472	0.0915	0.1021	0.2710	0.2829	1.5828	1.7753

5 Conclusion

In this paper we propose a meshfree solver for electromagnetics time-domain simulations. The method is appealing and avoids to deal with spatial meshes. The improved fast Gauss transform has been adopted to reduce the computational effort of the sums employed in the discrete formulation preserving a good accuracy level. We present first results able to speed the computation of the standard formulation with the aim to adopt the approach to describe in a fast and accurate way the effects of electromagnetic radiation on human tissue.

Acknowledgements.
The authors acknowledge support by INdAM–GNCS Project 2019 *”Kernel-based approximation, multiresolution and subdivision methods and related applications”*. This research has been accomplished within RITA (Research ITalian network on Approximation).

References

1. G.Ala and E.Francomano, A marching-on in time meshless kernel based solver for full-wave electromagnetic simulation, Numerical Algorithms, Vol. 62(4), 2013, pp. 541–558 (2013).
2. G.Ala and E.Francomano, Numerical Investigations of an Implicit Leapfrog Time-Domain Meshless Method, Journal on Scientific Computing, Vol. 62(3), pp. 898–912 (2014).
3. G.Ala, E.Francomano and S.Ganci, Unconditionally stable meshless integration of time-domain Maxwell's curl equations, Applied Mathematics and Computation, Vol. 255, pp.157–164 (2015).
4. B.Fornberg and N.Flyer, A primar on radial basis functions with applications to the geosciences, CBMS-NSF, 87, SIAM (2015).
5. E.Francomano and M.Paliaga, Highlighting numerical insights of an efficient SPH method, Applied Mathematics and Computation, Vol. 339, pp. 899–915 (2018).
6. E.Francomano, F.M.Hilker, M.Paliaga and E.Venturino, Separatrix reconstruction to identify tipping points in an eco-epidemiological model, Applied Mathematics and Computation, Vol. 318, pp. 80–91 (2018).
7. E.Francomano and M.Paliaga, Detecting tri-stability of 3D models with complex attractors via meshfree reconstruction of invariant manifolds of saddle points, Mathematical Methods in the Applied Sciences, Vol. 41 (17), pp. 7450–7458 (2018).
8. R.A.Gingold and J.J.Monaghan, Smoothed particle hydrodynamics: theory and application on spherical stars, Monthly Notices Roy. Astronom. Soc., Vol. 181, pp. 375–389 (1977).
9. L.Greengard and J.Strain, The fast Gauss transformation, SIAM J. Sci. Statist. Comput., Vol. 12(1), pp. 79–94 (1991).
10. S.M.Harrison, P. W.Cleary and M.Sinnott, Investigating mixing and emptying for aqueous liquid content from the stomach using a coupled biomechanical-SPH model, Food Function 9 (6), 3202-3219 (2018).
11. G.R.Liu and M.B.Liu, Smoothed Particle Hydrodynamics - A Mesh-Free Particle Method, World Scientific Publishing, Singapore (2003).
12. M.B.Liu, and G.R.Liu, Smoothed particle hydrodynamics (SPH): An overview and recent developments, Archives of Comput. Methods in Engineering, Vol. 17(1), pp. 25–76 (2010).
13. L.B.Lucy, A numerical approach to the testing of fusion process, Astron J, Vol. 82, pp. 1013–1024, (1977).
14. S.Ma, X.Zhang, Y.Lian and X.Zhou, Simulation of high explosive explosion using adaptive material point method, Computer Modeling in Engineering and Sciences, Vol. 39, pp. 101–123 (2009).
15. JJ.Monaghan, An introduction to SPH, Comput Phys Commun, Vol. 48, pp. 89–96 (1988).
16. C.Ulrich, M.Leonardi and T.Rung, Multi-physics SPH simulation of complex marine-engineering hydrodynamic problems Ocean Engineering, Vol. 64, pp. 109–121 (2013).

17. C.Yang, R.Duraiswami, N.A.Gumerov and L.S.Davis, Improved fast Gauss transform and efficient kernel density estimation, Proceedings Ninth IEEE International Conference on Computer Vision, (2003).
18. C.Yang, R.Duraiswami and L.S.Davis. Efficient kernel machines using the improved fast Gauss transform, Advances in neural information processing systems, (2004).
19. D.M.Sullivan, Electromagnetic simulation using the FDTD method, IEEE PRESS (2000).